Journal of Psychiatric Research 136 (2021) 351–357

Contents lists available at ScienceDirect

Journal of Psychiatric Research

journal homepage: www.elsevier.com/locate/jpsychires

Retinal dysfunctions in regular tobacco users: The retina as a window to the reward circuit in addictive disorders

Mathilde Dartois [a], Nicolas Haudiquet [a], Eliane Albuisson [b,c,d,g], Karine Angioi-Duprez [e,g], Raymund Schwan [a,f,g], Vincent Laprévote [a,f,g], Thomas Schwitzer [a,f,g,*]

[a] Pôle Hospitalo-Universitaire de Psychiatrie d'Adultes et d'Addictologie du Grand Nancy, Centre Psychothérapique de Nancy, Laxou, France
[b] CHRU-Nancy, DRCI, Département MPI, Unité de Méthodologie, Data management et Statistique UMDS, F-54000, Nancy, France
[c] Université de Lorraine, Faculté de Médecine, InSciDenS, F-54000, Nancy, France
[d] Université de Lorraine, CNRS, IECL, F-54000, Nancy, France
[e] Service d'Ophtalmologie, CHRU Nancy, Nancy, France
[f] INSERM U1114, Fédération de Médecine Translationnelle de Strasbourg, Département de Psychiatrie, Centre Hospitalier Régional Universitaire de Strasbourg, Strasbourg, France
[g] Faculté de Médecine, Université de Lorraine, Vandœuvre-lès-Nancy, France

ARTICLE INFO

Keywords:
Tobacco
Nicotine
Retina
Electroretinogram
Synaptic transmission
Reward circuit

ABSTRACT

The nicotine contained in tobacco is a neuromodulator which affects neurotransmission within the brain. The retina is an easy way to study central synaptic transmission dysfunctions in neuropsychiatric disorders. The purpose of this study is to assess the impact of regular tobacco use on retinal function using pattern (PERG), flash (fERG) and multifocal (mfERG) electroretinogram (ERG).

We recorded PERG, fERG and mfERG for 24 regular tobacco users and 30 healthy non-smoking subjects. The protocol was compliant with International Society for Clinical Electrophysiology of Vision standards. The amplitudes and peak times (PT) of P50, N95 waves (PERG), a-, b- and oscillatory potentials (fERG), and N1, P1, N2 (mfERG) were evaluated.

Compared to non-smokers, the results (Mann–Whitney *U* test, Bonferroni correction) for tobacco users suggested a significant increase of ~ 1 ms in the PT of light-adapted 3.0 fERG b-wave ($p = 0.002$). Using mfERG, we observed the following increases in tobacco users: in ring 3 for P1 PT of ~1,5 ms and in ring 5 for P1 PT of ~ 1 ms and for N2 PT of ~ 1 ms ($p = 0.002$, $p = 0.002$ and $p = 0.006$).

It is our hypothesis that these results reflect the consequences of regular tobacco use on retinal synaptic transmission, and more specifically on dopaminergic and cholinergic transmission. We deduce that the retina may provide a crucial site of investigation for neurotransmission modulation of the reward circuit in regular tobacco users.

1. Introduction

Today, the retina is used as a window into the brain when investigating neurotransmission modulations in neuropsychiatric and addictive disorders (Lavoie et al., 2014; London et al., 2013; Schwitzer et al., 2019). The retina is an anatomical and developmental extension of the central nervous system (Hoon et al., 2014). It is a complex neural network organized into several layers of specialized neurons which share similar anatomical and functional properties with brain neurons (Hoon et al., 2014). In the brain, dopamine and acetylcholine are neuromodulators targeted by the regular use of nicotine (Pistillo et al., 2015). The retina also contains dopamine and acetylcholine. In the retina, amacrine cells have dopaminergic activity, and dopaminergic receptors are found in the bipolar, horizontal, ganglion and photoreceptor cells (Hoon et al., 2014; Nguyen-Legros et al., 1997). Dopamine plays a role in the retina's circadian clock and serves as a regulator of high-acuity and light-adapted vision. Acetylcholine can be detected in the ganglion, bipolar and starburst amacrine cells, and is involved in

* Corresponding author. Psychotherapic Center of Nancy 1, rue du Docteur Archambault Laxou, F-54 521, France.
E-mail addresses: mathildedartois33@gmail.com (M. Dartois), haudiquet.n@live.fr (N. Haudiquet), eliane.albuisson@univ-lorraine.fr (E. Albuisson), karine.angioi@univ-lorraine.fr (K. Angioi-Duprez), raymund.schwan@univ-lorraine.fr (R. Schwan), Vincent.laprevote@cpn-laxou.com (V. Laprévote), thomas.schwitzer@univ-lorraine.fr (T. Schwitzer).

https://doi.org/10.1016/j.jpsychires.2021.02.023
Received 12 November 2020; Received in revised form 20 January 2021; Accepted 8 February 2021
Available online 13 February 2021

regulating the release of neurotransmitters in the retina (Dmitrieva et al., 2007; Hoon et al., 2014; Keyser et al., 2000; Strang et al., 2003).

Regular tobacco use is a major public health concern. It is a risk factor for mortality from such medical causes as cardiovascular diseases, chronic obstructive pulmonary disease and lung cancer (Brandon and Lam, 1983; Dowling and Ehinger, 1978; Ezzati and Lopez, 2003; Fielding, 2010). The main psychoactive substance found in tobacco is nicotine, a stimulant alkaloid making up 95%–97% of the total alkaloid content (Khalki et al., 2013). In the brain, the nicotine in tobacco modulates dopaminergic and nicotinic acetylcholinergic pathways. Nicotine increases dopamine in the ventral striatum and has a direct effect on nACHRs in the reward circuit, changing neuronal function by interrupting the transmission of endogenous acetylcholine (Gotti et al., 2007; Hoon et al., 2014). Like the brain, retinal neurotransmission is affected by tobacco use. Varghese et al. suggest that nicotine alters amacrine and cone bipolar cells that express nicotinic receptors (Varghese et al., 2011). Studying retinal processing is therefore a good way of exploring the effects of tobacco use on neurotransmission in the brain and the reward circuit in particular (Maziade and Silverstein, 2020; Schwitzer et al., 2017b).

A helpful tool for studying neuroretinal processing is the electroretinogram (ERG; (Holder et al., 2010; Hoon et al., 2014). ERG is an objective and electrophysiological technique which records the electrical biopotential of the retinal cells' response to light stimulation (Bach et al., 2013; Hood et al., 2012; McCulloch et al., 2015). Flash ERG (fERG) evaluates the function of photoreceptors (cones and rods), ON-bipolar and Müller cells complex and amacrine cells. Pattern ERG (PERG) evaluates ganglion cell and macular function, and multifocal ERG (mfERG) examines the spatial properties of central retinal cone function (Fig. 1).

In humans, several studies have looked at the chronic effects of tobacco smoking on retinal processing using PERG and mfERG (Fig. 2 (Abdelshafy and Abdelshafy, 2020; El-Shazly et al., 2018; 2017; Sobacı et al., 2013);. The results of these studies suggest that regular tobacco use alters retinal function. Using PERG, Abdelshafy et al. showed an increase in N95 peak time and a decrease in N95 amplitude for a group of chronic tobacco smokers—defined as those smoking at least 15 cigarettes per day for 10 years—compared to healthy non-smoking subjects. Previously, El-Shazly et al. found an increase in N95 peak time and a decrease in N95 amplitude in a group of active tobacco smokers (at least 10 cigarettes per day for 10 years) compared with a group of passive smokers (healthy participants in close contact with smokers; (El-Shazly et al., 2017). These studies suggest that cigarette smoking has an impact on ganglion cell response. Using mfERG, one study compared the effects of tobacco smoking for a group of active smokers—defined as those consuming at least one pack per day over the past five years—and a healthy control group. The study's authors only looked at central responses (central hexagon 6°) and did not find significant differences for N1 and P1 peak times and amplitudes (Sobacı et al., 2013). Another study used mfERG to compare an active and passive smoker group and found a significant decrease in P1 amplitude (<2°, ring 1) among active smokers, as well as an increase in P1 peak time (<2°, ring 1) and lower amplitude ratios (El-Shazly et al., 2018).

To the best of our knowledge, 1) no studies have used fERG to

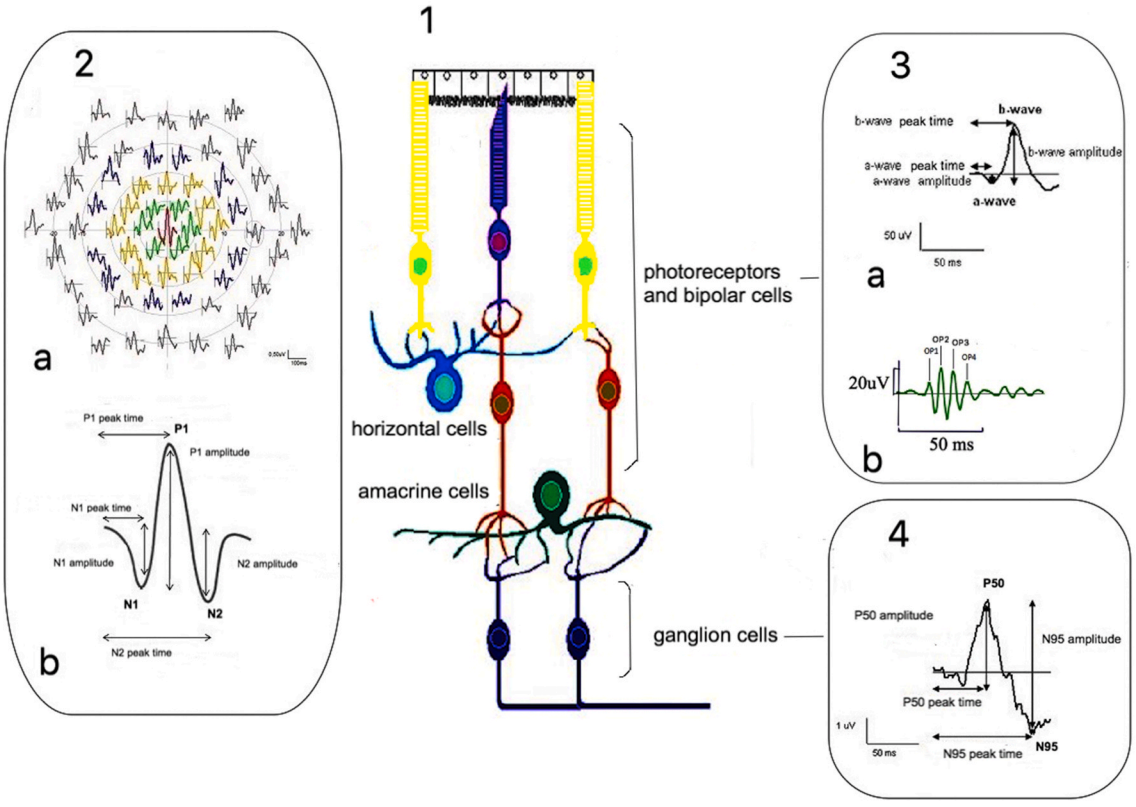

Fig. 1. 1. Schematic organization of the retina with cells(based on Schwitzer et al. 2017b)
2a. Multifocal ERG (mfERG) global traces with concentric rings which represent the five retinal regions from the central fovea to the peripheral retina:ring 1(<2°), ring 2(2-5°), ring 3(5-10°), ring 4(10-15°) and ring 5(>15°)
2b. Typical isolated mfERG wave
3a.Typical light-adapted 3.0 fERG trace
3b. Typical dark-adapted oscillatory potential trace
4. Typical PERG trace
The arrows represent the way the parameters are measured, namely amplitude and peak time

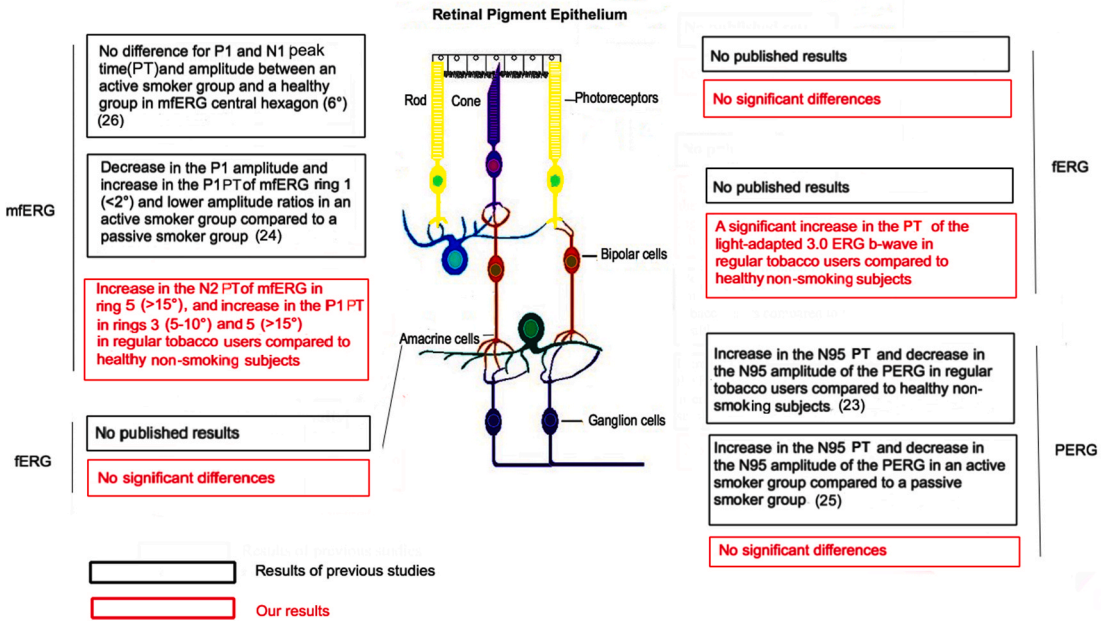

Fig. 2. Schematic representation of the retina with results of previous studies of tobacco users(based on Schwitzer et al., 2017a)

compare regular tobacco users and healthy subjects, 2) no studies have compared oscillatory potentials (OPs) in regular smokers and healthy subjects, and 3) no studies have performed a complete retinal exploration using PERG, fERG and mfERG to evaluate the effects of regular tobacco use on human retinal function as compared to that of a healthy non-smoking group. The aim of our study was to use PERG, fERG and mfERG to carry out a complete evaluation of retinal neurons in regular tobacco users and compare this with healthy non-smoking control subjects.

2. Materials and methods

2.1. Population and ethics statement

Regular tobacco users (n = 24) and age- and sex-matched healthy drug-naive controls (n = 30) were recruited from among the general population through a special press campaign, and data were collected from February 11, 2014 to June 03, 2019.

This study is part of a wider project—Causa Map (NCT02864680)—which researched the impact of regular cannabis use on the visual system. The protocol has been described in previous studies (Lucas et al., 2019; Polli et al., 2020; Schwitzer et al, 2017, 2018, 2019).

Briefly, volunteers underwent a full psychiatric evaluation. None of the participants had DSM-IV diagnosis of Axis I disorders evaluated by MINI. Participants signed consent forms detailing all aspects of the research. All participants received a payment of €100 in the form of gift vouchers. The study protocol met the requirements of the Helsinki Declaration and was approved by the Ethics Committee of Nancy University Hospital.

2.2. Inclusion criteria, and clinical and biological assessments

The inclusion criteria for the tobacco group were tobacco use for at least 12 months, a low to very high smoking dependence according to the Fagerström test, an abstention from cannabis use for at least 12 months, a negative urine toxicology screen for cannabis, and no DSM-IV diagnosis of an Axis I disorder.

The general inclusion criteria for the healthy control subjects and for all participants were described in previous studies (Polli et al., 2020; Schwitzer et al., 2017, 2018, 2020).

2.3. Experimental protocol

PERGs, fERGs and mfERGs were performed in accordance with International Society for Clinical Electrophysiology of Vision (ISCEV) standards (Bach et al., 2013; Hood et al., 2012; McCulloch et al., 2015). The MonPackOne system (Metrovision, Pérenchies, France) was used for stimulation, recording and analysis. Electrical signals were recorded simultaneously from both eyes. Averaged retinal responses were first obtained from each eye, and then the values for given parameters (peak time and amplitude) were averaged over both eyes to allow analysis. Electrical signals were recorded on non-dilated (PERG) and dilated pupils (fERG, mfERG, Tropicamide 0.5%) using DTL electrodes (Metrovision, Pérenchies, France) placed at the bottom of the conjunctival sac. Pupil sizes were noted before fERG and after mfERG recordings, and remained systematically constant throughout the testing period. Ground and reference electrodes were attached to the forehead and external canthi.

Pattern (PERG), flash (fERG) and multifocal electroretinogram (mfERG).

PERG protocol was previously described in (Schwitzer et al, 2017, 2018), fERG protocol in (Polli et al., 2020; Schwitzer et al., 2018) and mfERG protocol in (Schwitzer et al., 2020).

2.4. Analysis

The PERG, fERG and mfERG data were analyzed using Ophthalmic Monitor (Metrovision, Pérenchies, France). This analysis was carried out with the experimenter blind to which group the subject whose data had been recorded belonged to (tobacco user or control). Two main components are usually described on a typical PERG trace: an electropositive component, P50, followed by an electronegative component, N95. N95 is believed to reflect the response of retinal ganglion cells. P50 reflects the response of the retinal ganglion cells and macular photoreceptors. Two main parameters are derived from P50 and N95, referred to as the amplitude, measured in microvolts (μV), and the peak time, measured in milliseconds (ms). N95 amplitude is measured from the trough of N95 to the peak of P50. P50 amplitude is measured from the trough of the inconstant N35—or from the baseline—to the peak of P50. Peak time denotes the time taken to reach the maximum N95 and P50 amplitudes (Fig. 1).

Conversely, the two main components usually described on a typical fERG are an electronegative component, the a-wave, followed by an electropositive component, the b-wave. The a-wave is not detected in the dark-adapted 0.01 ERG response because it is masked by the b-wave. A-waves are attributed to the retinal photoreceptors and b-waves are attributed to the retinal bipolar cells, which are postsynaptic to photoreceptors. Two main parameters are derived from a- and b-waves, referred to as the amplitude measured in microvolts (μV) and the peak time measured in milliseconds (ms). The a-wave amplitude is measured from the baseline to the trough of the a-wave. The b-wave amplitude is measured from the trough of the a-wave to the peak of the b-wave. Peak time denotes the time taken to reach the maximum a- and b-wave amplitudes (Fig. 1).

The mfERG responses were averaged over five retinal regions: <2°, 2°–5°, 5°–10°, 10°–15° and >15°. Three main components are usually described on a typical mfERG trace: a first negative wave known as N1, followed by an electropositive component, P1, and then a second negative wave, N2. Two main parameters are derived from N1, P1 and N2, referred to as the amplitude measured in microvolts (μV) and the peak time measured in ms. The amplitude of N1 was measured from the baseline to the trough of N1. The amplitudes of P1 and N2 are the trough-to-peak amplitudes, measured respectively from the trough of N1 to the peak of P1, and from the peak of P1 to the trough of N2. Peak time denotes the time taken to reach the maximum N1, P1 and N2 amplitudes (Fig. 1). Responses from each eye were recorded. The analysis was carried out after averaging the responses for both eyes.

2.5. Statistical analysis

Depending on their nature and the non-parametric distribution of the quantitative variables included in the analyses, a Mann–Whitney *U* test and Chi-square test were used when appropriate to compare the tobacco user and control groups. When tests were performed on parameters extracted from the same ERG trace, ie "dark-adapted 3.0 ERG or scotopic oscillatory potentials", to name a few, and accordingly to a possible dependence, a Bonferroni correction on the alpha risk was performed for the tests concerning this same trace. When tests were used on parameters extracted from separated ERG traces, we considered them as nondependent and no correction was performed. For mfERG, we applied the same methodology concerning the alpha risk. Statistical analyses were performed using IBM SPSS Statistics 22.0 (IBM corp.).

3. Results

3.1. Demographic and substance use characteristics

The demographic and substance use characteristics of the participants are described in Table 1. There was no relevant difference between the controls and tobacco users in terms of gender (p = 0.143), age (p = 0.065) and years of education (p = 0.465), but differences were noted between the groups in terms of alcohol use, which was higher among tobacco users (p = 0.006 for average alcohol consumption/week, p = 0.025 for AUDIT score). Based on the Fagerström test, of the 24 tobacco users, 12 were slightly dependent, 8 were mildly dependent and 4 were highly dependent.

3.2. ERG parameters

Table 2 summarizes all the results for the PERG, fERG and mfERG measurements. Only significant results are given here.

3.3. fERG: light-adapted 3.0 ERG

The median and interquartile range of the b-wave peak time was 36.75 ms (35.96:37.09) for tobacco users versus 35.85 ms (34.95:36.30) for the controls. The b-wave peak time was significantly increased of approximatively 1 ms in tobacco users (p = 0.002; Mann–Whitney test).

Table 1
Demographic and substance use characteristics of the participants.

	Tobacco users (n = 24)	Controls (n = 30)	*P*-value
Gender (male/female)[a,d]	13/11	22/8	*p = 0.143*
Age (years)[b,c]	28 (23.5–30)	24 (22.75–27.25)	*p = 0.065*
Education (years)[b,c]	14 (13–16.75)	15 (14–16)	*p = 0.465*
Average number of alcohol uses/week[b,c]	4 (2–6)	1 (0–3.25)	*p = 0.006*
Alcohol Use Disorders Identification Test (AUDIT) scores[b,c]	4 (3–6)	3 (1–4.25)	*p = 0.025*
Fagerström Test scores[b] **(n=24)**	4.5 (3–5)	–	–
Average number of cigarettes/day[b] **(n=24)**	11 (7.75–17.75)	–	–
Average number pack-years of cigarettes[b] **(n=22)**	4.65 (2.875–10.649)	–	–
Age of first tobacco use[b]**(n=22)**	18.5 (16–20)	–	–

[a] Categorical variable represented as frequencies.
[b] Quantitative variable represented as median and interquartile range[b].
[c] Mann-Whitney *U* test.
[d] Chi-Square test [d].

3.4. mfERG

In ring 3 (5°–10°): The median and interquartile range of the P1 peak time for 5°–10° was 44.00 ms (42.99:45.09) for tobacco users and 42.53 ms (41.88:43.50) for the controls. The P1 peak time was significantly increased of approximatively 1,5 ms in tobacco users (p = 0.002; Mann–Whitney test).

In ring 5 (>15°): The median and interquartile range of the P1 peak time for >15° was 43.10 ms (42.59:44.14) for tobacco users and 42.03 ms (41.63:42.76) for the controls. The P1 peak time was significantly increased of approximatively 1 ms in tobacco users (p = 0.002; Mann–Whitney test).

The median and interquartile range of the N2 peak time for >15° was 61.68 ms (60.69:62.70) for tobacco users and 60.62 ms (59.10:61.06) for the controls. The N2 peak time was significantly increased of approximatively 1 ms in tobacco users (p = 0.006; Mann–Whitney test).

4. Discussion

These results suggest that regular tobacco use impacts both the function of the retinal bipolar cells and the spatial properties of the retinal cone system. Firstly, delayed retinal signaling at the bipolar cell level was found in regular tobacco users, observed as an increase of ~1 ms in the light-adapted 3.0 fERG b-wave peak time. This delay was also detected in the mfERG measurements. Compared with healthy subjects, we observed: an increase in P1 peak time of ~1,5 ms (ring 3), an increase in P1 peak time of ~1 ms (ring 5) and an increase in N2 peak time of ~1 ms (ring 5). No significant anomaly was found in either the rod bipolar or ganglion cells.

It is our hypothesis that these results demonstrate modulation of the retinal dopaminergic pathways. We believe that the b-wave of the light-adapted 3.0 fERG has a dopaminergic implication and could be an indicator of dopamine modulation of the reward circuit in addictive disorders. Several arguments support this hypothesis. Among regular tobacco users, an increase of ~1 ms in the b-wave peak time of the light-adapted 3.0 fERG was observed. We know that chronic use of nicotine, the main addictive component of tobacco, affects the reward system by modulating dopamine release in the nucleus accumbens (Svensson,

Table 2
Electroretinogram (ERG) parameters of the participants.

	Tobacco users (n = 24)	Controls (n = 30)	*P*-Value
Pattern Electroretinogram (PERG)			
N95 peak time (ms)[a,b]	92.90 (86.25:100.35)	89.38 (84.50:91.60)	*p= 0.050, NS*
N95 amplitude (μV)[a,b]	−3.70 (−4.60: 2.80)	−3.73 (−4.49: 3.11)	*p = 0.554, NS*
P50 peak time (ms)[a,b]	51.75 (47.75:56.15)	48.65 (47.20:51.30)	*p = 0.136, NS*
P50 amplitude (μV)[a,b]	2.60 (2.30:3.30)	2.35 (2.15:2.69)	*p = 0.062, NS*
Flash Electroretinogram (fERG)			
Dark-adapted 0.01 ERG			
a-wave peak time (ms)[a]	37.95 (36.20:39.25)	37.95 (36.65:39.26)	*p = 0.619, NS*
a-wave amplitude (μV)[a]	−6.93 (−10.35: 4.58)	−8.15 (−11.01: 4.78)	*p = 0.537, NS*
b-wave peak time (ms)[a]	79.80 (77.10:88.68)	80.68 (77.58:84.90)	*p = 0.801, NS*
b-wave amplitude (μV)[a]	125.75 (102.75:172.88)	132.75 (118.63:158.63)	*p = 0.508, NS*
Dark-adapted 3.0 ERG			
a-wave peak time (ms)[a,b]	24.35 (23.90:24.80)	23.90 (23.45:24.80)	*p = 0.244, NS*
a-wave amplitude (μV)[a,b]	−97.45 (−111.00: 81.00)	−106.75 (−112.50: 90.94)	*p = 0.199, NS*
b-wave peak time (ms)[a,b]	47.35 (46.00:50.05)	46.68 (45.60:48.70)	*p = 0.235, NS*
b-wave amplitude (μV)[a,b]	162.00 (135.50:183.00)	164.50 (153.25:199.88)	*p = 0.222, NS*
Scotopic Oscillatory Potentials (OPs)			
OP1 peak time (ms)[a]	21.40 (21.10:21.70)	21.10 (20.80:22.00)	*p = 0.542, NS*
OP1 amplitude (μV)[a]	−15.95 (−18.42: 11.73)	−17.50 (−20.59: 15.20)	*P = 0.036, NS*
OP2 peak time (ms)[a]	24.70 (24.40:25.00)	24.70 (24.40:25.60)	*p = 0.553, NS*
OP2 amplitude (μV)[a]	33.90 (25.39:38.89)	37.60 (33.23:45.40)	*p = 0.049, NS*
OP3 peak time (ms)[a]	27.90 (27.60–28.50)	28.20 (27.60:28.88)	*p = 0.516, NS*
OP3 amplitude (μV)[a]	−32.30 (−38.34: 24.41)	−39.45 (−42.60: 31.16)	*p = 0.042, NS*
OP4 peak time (ms)[a]	31.35 (30.90:32.05)	31.50 (31.20:32.41)	*p = 0.251, NS*
OP4 amplitude (μV)[a]	28.03 (18.41:33.47)	31.88 (26.84:36.46)	*p = 0.095, NS*
Light-adapted 3.0 ERG			
a-wave peak time (ms)[a]	18.60 (18.15:19.50)	18.60 (18.15:19.05)	*p = 0.324, NS*
a-wave amplitude (μV)[a]	−10.43 (−12.5: 8.39)	−10.75 (−12.63:9.31)	*p = 0.394, NS*
b-wave peak time (ms)[a]	**36.75 (35.96:37.09)**	**35.85 (34.95:36.30)**	***p = 0.002, S***
b-wave amplitude (μV)[a]	43.58 (39.72:52.13)	47.98 (39.55:51.94)	*p = 0.814, NS*
Multifocal Electroretinogram(mfERG)			
<2° (ring 1)			
N1 amplitude (μV)[a,c]	−449.00 (-757.75: 357.75)	−459.50 (-549.00: 419.88)	*p = 0.963, NS*
N1 peak time (ms)[a,c]	26.53 (24.96:28.31)	26.37 (25.09:28.06)	*p = 0.935, NS*
P1 amplitude (μV)[a,c]	803.75 (682.25:1229.3)	923.50 (763.00:1068.38)	*p = 0.526, NS*
P1 peak time (ms)[a,c]	50.18 (49.13:52.71)	49.83 (47.94:51.56)	*p = 0.324, NS*
N2 amplitude (μV)[a,c]	−735.25 (-994.63: 639.88)	−940.25 (-1181.63: 716.75)	*p = 0.146, NS*
N2 peak time (ms)[a,c]	72.42 (70.64:74.74)	70.28 (67.70:72.35)	*p = 0.012, NS*
2–5° (ring 2)			
N1 amplitude (μV)[a,c]	−249.00 (-309.50: 214.00)	−245.50 (-319.50: 207.75)	*p = 0.869, NS*
N1 peak time (ms)[a,c]	26.07 (24.94:27.21)	25.30 (24.39:26.26)	*p = 0.169, NS*
P1 amplitude (μV)[a,c]	491.00 (435.13:598.13)	495.25 (433.50:550.63)	*p = 0.925, NS*
P1 peak time (ms)[a,c]	45.83 (44.56:47.46)	45.25 (43.86:46.33)	*p = 0.142, NS*
N2 amplitude (μV)[a,c]	−406.50 (-497.75: 276.75)	−403.00 (-459.13: 349.63)	*p = 0.690, NS*
N2 peak time (ms)[a,c]	67.45 (65.01:71.04)	64.70 (62.10:65.76)	*p = 0.011, NS*
5–10° (ring 3)			
N1 amplitude (μV)[a,c]	−203.50 (-227.13: 154.62)	−184.50 (-232.62: 149.25)	*p = 0.446, NS*
N1 peak time (ms)[a,c]	24.75 (23.95:25.66)	24.38 (23.68:25.06)	*p = 0.201, NS*
P1 amplitude (μV)[a,c]	362.75 (334.13:430.00)	371.25 (346.38:462.25)	*p = 0.503, NS*
P1 peak time (ms)[a,c]	**44.00 (42.99:45.09)**	**42.53 (41.88:43.50)**	***p = 0.002, S***
N2 amplitude (μV)[a,c]	−326.00 (-386.13: 281.13)	−327.75 (-394.88: 285.38)	*p = 0.805, NS*
N2 peak time (ms)[a,c]	64.20 (61.93–66.40)	61.70 (60.09:64.76)	*p = 0.054, NS*
10–15° (ring 4)			
N1 amplitude (μV)[a,c]	−166.50 (-203.75: 134.38)	−148.25 (-197.50: 131.72)	*p = 0.398, NS*
N1 peak time (ms)[a,c]	24.70 (23.59:25.63)	23.98 (23.44:24.71)	*p = 0.189, NS*
P1 amplitude (μV)[a,c]	350.50 (298.00:412.63)	356.75 (311.50:406.75)	*p = 0.981, NS*
P1 peak time (ms)[a,c]	43.13 (42.38:44.21)	42.25 (41.54:42.66)	*p = 0.009, NS*
N2 amplitude (μV)[a,c]	−327.25 (-381.63: 260.63)	−294.50 (-344.13: 269.62)	*p = 0.519, NS*
N2 peak time (ms)[a,c]	62.05 (60.51:62.98)	60.88 (59.15:62.05)	*p = 0.105, NS*
>15° (ring 5)			
N1 amplitude (μV)[a,c]	−153.25 (-178.50: 135.38)	−148.50 (-176.25:116.88)	*p = 0.439, NS*
N1 peak time (ms)[a,c]	24.60 (23.79:25.40)	24.00 (23.64:24.56)	*p = 0.110, NS*
P1 amplitude (μV)[a,c]	348.25 (298.75:402.25)	332.00 (297.75:382.00)	*p = 0.392, NS*
P1 peak time (ms)[a,c]	**43.10 (42.59:44.14)**	**42.03 (41.63:42.76)**	***p = 0.002, S***
N2 amplitude (μV)[a,c]	−303.50 (-368.50: 272.63)	−300.75 (-340.88: 269.88)	*p = 0.725, NS*
N2 peak time (ms)[a,c]	**61.68 (60.69:62.70)**	**60.62 (59.10:61.06)**	***p = 0.006, S***

NS: non significant.
S: significant.
[a] Quantitative variable represented as median and interquartile range.
[b] Tobacco users n = 23.
[c] Tobacco users and controls n = 22.

2002). As retinal bipolar cells -at the origin of the b-wave- contain dopamine and dopaminergic receptors (Nguyen-Legros et al., 1997), we surmise that nicotine has an effect on the function of these cells. A delayed bipolar cell response as demonstrated by an increase of ~1 ms in the light-adapted 3.0 fERG b-wave peak time has also been observed by our group in regular cannabis users (Schwitzer et al., 2018). Similarly to tobacco use, regular cannabis use produces modulation of dopamine

levels in the reward circuit (Gardner, 2005). Tetrahydrocannabinol (THC) causes increased dopamine release by activating cannabinoid CB1 receptors (Bloomfield et al., 2016; Bossong et al., 2009). Taken together, these results suggest that the fERG light-adapted b-wave could provide information on dopamine modulation in the reward system in cases of substance use disorders. In the brain, regular tobacco and cannabis use are associated with a dopamine deficiency, which can also be found in the retina and which is characterized by an increase in the light-adapted 3.0 b-wave peak time. Previous findings support a link between lower levels of dopamine and an increased b-wave. In tryptophan hydroxylase 2 knock-in (Tph2-KI) mice with an approximately 80% decrease in brain serotonin and dopamine, an increase in the b-wave peak time of the light-adapted fERG was observed (Lavoie et al., 2014). For patients with Parkinson's disease, a neurological disorder associated with a dopamine deficiency, a significantly increased b-wave peak time, such as we found in regular tobacco and cannabis users, has been observed (Ikeda et al., 1994).

Our results observed with mfERG are consistent with those observed with fERG since increased peak times were also found. They suggest that regular tobacco consumption has an effect on P1 peak time ring 3 and 5, and on N2 peak time ring 5. Among cannabis users, we previously found an increase in the N2 peak time in rings 1 and 2 and an increase in the P1 peak time in rings 2, 3 and 4 (Schwitzer et al, 2019). We have also observed significant correlations between the number of cigarettes per day and N2 peak time in ring 1 ($p = 0.01$) and P1 peak time in ring 4 ($p = 0.036$) among cannabis users (Schwitzer et al, 2019). Here, we also observed an increase in N2 peak time (ring 1) of ~2 ms and P1 peak time (ring 4) of ~1 ms in regular tobacco users, although they were no significant.

In comparison with the retinal alterations found in cannabis users (Lucas et al., 2019; Polli et al., 2020; Schwitzer et al, 2018, 2019), we assume that we found both similar and different retinal dysfunctions in regular tobacco users. Several retinal alterations are specific to regular cannabis use, such as the increase in the PERG N95 peak time, which was not found in tobacco users. We conjecture that this anomaly involves neurotransmission modulations specific to cannabis use, and glutamatergic modulations in particular (Bernardin et al., 2017; Schwitzer et al., 2019). On the other hand, we maintain that some retinal dysfunctions are found in those who regularly use any addictive substance such as tobacco or cannabis, since such regular use modulates the reward circuit, and central dopaminergic neurotransmission in particular. In both regular cannabis and tobacco use, we found similar retinal dysfunctions, which could be viewed as modulations of dopaminergic neurotransmission in the retina (Polli et al., 2020; Schwitzer et al., 2018). As the retina is a window to the brain, we deduce that these retinal dopaminergic modulations are a reflection of dopaminergic modulations in the brain.

Tobacco is also known to be a modulator of cholinergic neurotransmission, and we therefore contend that our results demonstrate a modulation of retinal cholinergic pathways. In the CNS, nicotine impacts nicotinic acetylcholine receptors (nACHRs) and alters neuronal function by interrupting the transmission of endogenous achetylcholine (Pistillo et al., 2015). In the retina, bipolar cells express nACHRs (Dmitrieva et al., 2007; Elgueta et al., 2015; Hoon et al., 2014; Keyser et al., 2000; Strang et al., 2003). Our results suggest that the function of bipolar cells is altered in tobacco users. These alterations could therefore be viewed as the effect of nicotine on nACHRs in bipolar cells and thus on retinal cholinergic transmission. Previous findings in animals support this hypothesis. Jurklies et al. found modifications in the b-wave under light- and dark-adapted conditions in cats treated with a cholinergic agonist (acetylcholine) or a muscarinic acetylcholine antagonist (scopolamine; (Jurklies et al., 1996). In humans, one previous study has looked at the acute effects of nicotine on the retina. Chewing-gum containing 2 mg or 4 mg of nicotine was administered to non-smoking adults 30 min before fERG testing (Varghese et al., 2011). The authors observed changes in the amplitudes of the light- and dark-adapted fERG b-waves and hypothesized that nicotine affects retinal responses via the nACHRs.

This study has several limitations. Cigarettes are composed of numerous addictive substances, and we assume here that nicotine is the main substance causing modulations of retinal synaptic transmission. In order to confirm the key role played by nicotine in these results, further studies should look only at chronic nicotine use. Another limitation is the alcohol consumption frequently observed in tobacco users (MacLean et al., 2018). This study found significant differences between the tobacco and control groups in terms of the number of units of alcohol consumed per week and their AUDIT score. The potentiating effect of these two substances (alcohol and tobacco) on neurotransmission, and dopaminergic neurotransmission in particular, cannot therefore be ruled out. Future studies should explore the isolated effect of the regular use of each substance on retinal function by comparing groups of tobacco-only and alcohol-only users. Furthermore, it would be interesting in future studies to compare with ERGs different populations of consumers, for example tobacco and cannabis users, to evaluate the sensitivity and specificity of the findings in each population.

To conclude, ERG measurements may be a relevant tool for studying neurotransmission abnormalities in cases of addictive disorders, and in particular, the effects of substance use on the reward system. In the future, ERG could one day be used to monitor the effects of pharmacological treatments for addictive disorders. fERG, PERG and mfERG are complementary retinal electrophysiological measures using different types of stimulations -flashes, checkerboards and hexagons-to study functional and spatial properties of several retinal neurons and may inform on different neurotransmission systems.

Author contributions

All the authors contributed to write the manuscript, concurred with the submission and have approved the final manuscript.

Funding

This study was supported by a French National Research Agency (ANR) Grant (ANR-12-SAMA-0016-01) and by the French Mission Interministérielle de Lutte Contre les Drogues et les Conduites Addictives (MILDECA). ANR and MILDECA have no role in design and conduct of the study; collection, management, analysis, and interpretation of the data; preparation, review, or approval of the manuscript; and decision to submit the manuscript for publication.

Ethical statement

The study protocol met the requirements of the Helsinki Declaration and was approved by the Ethics Committee of Nancy University Hospital. This study is part of a bigger project, Causa Map, which is researching the impact of regular cannabis use on the visual system.

Declaration of competing interest

All the authors declare that the research was conducted in the absence of any commercial or financial relationships that could be construed as a potential conflict of interest.

Acknowledgements

The authors thank the Ophtalmology staff of Nancy University Hospital and MetroVision for their contribution to this work. The authors also thank all members of the CAUSA MAP study group: Marc Borie, CHRU Nancy, France; Stéphanie Caharel, InterPsy, Université Lorraine, France; Paolo Di Patrizio, Université Lorraine, France; Philip Gorwood, Centre de Psychiatrie et Neurosciences, Paris, France; Coline Jeantet, InterPsy, Université Lorraine, France; Julien Krieg, INSERM

U1114, Université Strasbourg; Joëlle Lighezzolo-Alnot, InterPsy, Université Lorraine, France; Valérie Louis Dorr, CRAN CNRS UMR 7039, Nancy, France; Louis Maillard, CRAN CNRS UMR 7039, Nancy, France; Nicolas Ramoz, Centre de Psychiatrie et Neurosciences, Paris, France.

References

Abdelshafy, M., Abdelshafy, A., 2020. Functional and structural changes of the retinal nerve fiber layer and ganglion cell complex in heavy smokers. Clin. Ophthalmol. Auckl. NZ 14, 397–404. https://doi.org/10.2147/OPTH.S235892.

Bach, M., Brigell, M.G., Hawlina, M., Holder, G.E., Johnson, M.A., McCulloch, D.L., Meigen, T., Viswanathan, S., 2013. ISCEV standard for clinical pattern electroretinography (PERG): 2012 update. Doc. Ophthalmol. Adv. Ophthalmol. 126, 1–7. https://doi.org/10.1007/s10633-012-9353-y.

Bernardin, F., Schwan, R., Lalanne, L., Ligier, F., Angioi-Duprez, K., Schwitzer, T., Laprevote, V., 2017. The role of the retina in visual hallucinations: a review of the literature and implications for psychosis. Neuropsychologia 99, 128–138. https://doi.org/10.1016/j.neuropsychologia.2017.03.002.

Bloomfield, M.a.P., Ashok, A., Volkow, N.D., Howes, O.D., 2016. The Effects of Δ9-tetrahydrocannabinol (THC) on the Dopamine System, vol. 377. https://doi.org/10.1038/nature20153.

Bossong, M.G., van Berckel, B.N.M., Boellaard, R., Zuurman, L., Schuit, R.C., Windhorst, A.D., van Gerven, J.M.A., Ramsey, N.F., Lammertsma, A.A., Kahn, R.S., 2009. Delta 9-tetrahydrocannabinol induces dopamine release in the human striatum. Neuropsychopharmacol. Off. Publ. Am. Coll. Neuropsychopharmacol. 34, 759–766. https://doi.org/10.1038/npp.2008.138.

Brandon, C., Lam, D.M., 1983. L-glutamic acid: a neurotransmitter candidate for cone photoreceptors in human and rat retinas. Proc. Natl. Acad. Sci. U.S.A. 80, 5117–5121.

Dmitrieva, N.A., Strang, C.E., Keyser, K.T., 2007. Expression of alpha 7 nicotinic acetylcholine receptors by bipolar, amacrine, and ganglion cells of the rabbit retina. J. Histochem. Cytochem. Off. J. Histochem. Soc. 55, 461–476. https://doi.org/10.1369/jhc.6A7116.2006.

Dowling, J.E., Ehinger, B., 1978. The interplexiform cell system. I. Synapses of the dopaminergic neurons of the goldfish retina. Proc. R. Soc. Lond. B Biol. Sci. 201, 7–26.

Elgueta, C., Vielma, A.H., Palacios, A.G., Schmachtenberg, O., 2015. Acetylcholine induces GABA release onto rod bipolar cells through heteromeric nicotinic receptors expressed in A17 amacrine cells. Front. Cell. Neurosci. 9 https://doi.org/10.3389/fncel.2015.00006.

El-Shazly, A.A.E.-F., Farweez, Y.A.T., Elewa, L.S., Elzankalony, Y.A., Farweez, B.A.T., 2017. Effect of active and passive smoking on retinal nerve fibre layer and ganglion cell complex [WWW Document]. J. Ophthalmol. https://doi.org/10.1155/2017/6354025.

El-Shazly, A.A.E.-F., Farweez, Y.A.T., Elzankalony, Y.A., Elewa, L.S., Farweez, B.A.T., 2018. Effect OF smoking ON macular function and structure IN active smokers versus passive smokers. Retina Phila. Pa 38, 1031–1040. https://doi.org/10.1097/IAE.0000000000001632.

Ezzati, M., Lopez, A.D., 2003. Estimates of global mortality attributable to smoking in 2000. Lancet 362, 847–852. https://doi.org/10.1016/S0140-6736(03)14338-3.

Fielding, J.E, 2010. Smoking: health effects and control [WWW Document]. https://doi.org/10.1056/NEJM198508293130906. https://doi.org/10.1056/NEJM198508293130906.

Gardner, E.L., 2005. Endocannabinoid signaling system and brain reward: emphasis on dopamine. Pharmacol. Biochem. Behav. 81, 263–284. https://doi.org/10.1016/j.pbb.2005.01.032.

Gotti, C., Moretti, M., Gaimarri, A., Zanardi, A., Clementi, F., Zoli, M., 2007. Heterogeneity and complexity of native brain nicotinic receptors. Biochem. Pharmacol. 74, 1102–1111. https://doi.org/10.1016/j.bcp.2007.05.023.

Holder, G.E., Celesia, G.G., Miyake, Y., Tobimatsu, S., Weleber, R.G., 2010. International federation of clinical neurophysiology: recommendations for visual system testing. Clin. Neurophysiol. 121, 1393–1409. https://doi.org/10.1016/j.clinph.2010.04.010.

Hood, D.C., Bach, M., Brigell, M., Keating, D., Kondo, M., Lyons, J.S., Marmor, M.F., McCulloch, D.L., Palmowski-Wolfe, A.M., International Society For Clinical Electrophysiology of Vision, 2012. ISCEV standard for clinical multifocal electroretinography (mfERG) (2011 edition). Doc. Ophthalmol. Adv. Ophthalmol. 124, 1–13. https://doi.org/10.1007/s10633-011-9296-8.

Hoon, M., Okawa, H., Della Santina, L., Wong, R.O.L., 2014. Functional architecture of the retina: Development and disease. Prog. Retin. Eye Res. 42, 44–84. https://doi.org/10.1016/j.preteyeres.2014.06.003.

Ikeda, H., Head, G.M., Ellis, C.J., 1994. Electrophysiological signs of retinal dopamine deficiency in recently diagnosed Parkinson's disease and a follow up study. Vis. Res. 34, 2629–2638. https://doi.org/10.1016/0042-6989(94)90248-8.

Jurklies, B., Kaelin-Lang, A., Niemeyer, G., 1996. Cholinergic effects on cat retina in vitro: changes in rod- and cone-driven b-wave and optic nerve response. Vis. Res. 36, 797–816. https://doi.org/10.1016/0042-6989(95)00172-7.

Keyser, K.T., MacNeil, M.A., Dmitrieva, N., Wang, F., Masland, R.H., Lindstrom, J.M., 2000. Amacrine, ganglion, and displaced amacrine cells in the rabbit retina express nicotinic acetylcholine receptors. Vis. Neurosci. 17, 743–752. https://doi.org/10.1017/s095252380017508x.

Khalki, H., Navailles, S., Piron, C.L., De Deurwaerdère, P., 2013. A tobacco extract containing alkaloids induces distinct effects compared to pure nicotine on dopamine release in the rat. Neurosci. Lett. 544, 85–88. https://doi.org/10.1016/j.neulet.2013.03.047.

Lavoie, J., Illiano, P., Sotnikova, T.D., Gainetdinov, R.R., Beaulieu, J.-M., Hébert, M., 2014. The electroretinogram as a biomarker of central dopamine and serotonin: potential relevance to psychiatric disorders. Biol. Psychiatr. 75, 479–486. https://doi.org/10.1016/j.biopsych.2012.11.024.

London, A., Benhar, I., Schwartz, M., 2013. The retina as a window to the brain—from eye research to CNS disorders. Nat. Rev. Neurol. 9, 44–53. https://doi.org/10.1038/nrneurol.2012.227.

Lucas, A., Thirion, A., Schwan, R., Krieg, J., Angioi-Duprez, K., Laprevote, V., Schwitzer, T., 2019. Association between increased retinal background noise and co-occurrent regular cannabis and alcohol use. Prog. Neuro-Psychopharmacol. Biol. Psychiatry 89, 335–340. https://doi.org/10.1016/j.pnpbp.2018.10.002.

MacLean, R.R., Sofuoglu, M., Rosenheck, R., 2018. Tobacco and alcohol use disorders: evaluating multimorbidity. Addict. Behav. 78, 59–66. https://doi.org/10.1016/j.addbeh.2017.11.006.

Maziade, M., Silverstein, S.M., 2020. The place of the retina in psychiatry: uniting neurobiological and neurodevelopmental research with clinical research in psychiatric disorders. Schizophr. Res. 219, 1–4. https://doi.org/10.1016/j.schres.2020.03.028.

McCulloch, D., Marmor, M., Brigell, M., Hamilton, R., Holder, G., Tzekov, R., Bach, M., 2015. ISCEV Standard for full-field clinical electroretinography (2015 update). Doc. Ophthalmol. 130, 1–12. https://doi.org/10.1007/s10633-014-9473-7.

Nguyen-Legros, J., Simon, A., Caillé, I., Bloch, B., 1997. Immunocytochemical localization of dopamine D1 receptors in the retina of mammals. Vis. Neurosci. 14, 545–551. https://doi.org/10.1017/s0952523800012207.

Pistillo, F., Clementi, F., Zoli, M., Gotti, C., 2015. Nicotinic, glutamatergic and dopaminergic synaptic transmission and plasticity in the mesocorticolimbic system: focus on nicotine effects. Prog. Neurobiol. 124, 1–27. https://doi.org/10.1016/j.pneurobio.2014.10.002.

Polli, L., Schwan, R., Albuisson, E., Malbos, L., Angioi-Duprez, K., Laprevote, V., Schwitzer, T., 2020a. Oscillatory potentials abnormalities in regular cannabis users: amacrine cells dysfunction as a marker of central dopaminergic modulation. Prog. Neuro-Psychopharmacol. Biol. Psychiatry 110083. https://doi.org/10.1016/j.pnpbp.2020.110083.

Schwitzer, T., Henrion, M.-L., Sarre, D., Albuisson, E., Angioi-Duprez, K., Giersch, A., Lalanne, L., Schwan, R., Laprevote, V., 2020. Spatial localization of retinal anomalies in regular cannabis users: the relevance of the multifocal electroretinogram. Schizophr. Res. 219, 56–61. https://doi.org/10.1016/j.schres.2019.01.013.

Schwitzer, T., Schwan, R., Albuisson, E., Giersch, A., Lalanne, L., Angioi-Duprez, K., Laprevote, V., 2017. Association between regular cannabis use and ganglion cell dysfunction. JAMA Ophthalmol 135, 54–60. https://doi.org/10.1001/jamaophthalmol.2016.4761.

Schwitzer, T., Schwan, R., Angioi-Duprez, K., Giersch, A., Lalanne, L., Albuisson, E., Laprevote, V., 2018. Delayed bipolar and ganglion cells neuroretinal processing in regular cannabis users: the retina as a relevant site to investigate brain synaptic transmission dysfunctions. J. Psychiatr. Res. 103, 75–82. https://doi.org/10.1016/j.jpsychires.2018.04.021.

Schwitzer, T., Schwan, R., Angioi-Duprez, K., Lalanne, L., Giersch, A., Laprevote, V., 2019b. Cannabis use and human retina: the path for the study of brain synaptic transmission dysfunctions in cannabis users. Neurosci. Biobehav. Rev. 106, 11–22. https://doi.org/10.1016/j.neubiorev.2018.12.001.

Schwitzer, T., Schwan, R., Bubl, E., Lalanne, L., Angioi-Duprez, K., Laprevote, V., 2017b. Looking into the brain through the retinal ganglion cells in psychiatric disorders: a review of evidences. Prog. Neuro-Psychopharmacol. Biol. Psychiatry 76, 155–162. https://doi.org/10.1016/j.pnpbp.2017.03.008.

Sobacı, G., Musayev, S., Karslıoglu, Y., Gündoğan, F.Ç., Özge, G., Erdem, Ü., Bayer, 2013. The microstructural and functional changes in the macula of heavy habitual smokers. Int. Ophthalmol. 33, 461–466. https://doi.org/10.1007/s10792-013-9716-8.

Strang, C.E., Amthor, F.R., Keyser, K.T., 2003. Rabbit retinal ganglion cell responses to nicotine can be mediated by β2-containing nicotinic acetylcholine receptors. Vis. Neurosci. 20, 651–662. https://doi.org/10.1017/S0952523803206076.

Svensson, T.H., 2002. Effects of nicotine on the mesolimbic dopaminergic reward system in brain. Eur. Neuropsychopharmacol 12, 86. https://doi.org/10.1016/S0924-977X(02)80011-6.

Varghese, S.B., Reid, J.C., Hartmann, E.E., Keyser, K.T., 2011. The effects of nicotine on the human electroretinogram. Invest. Ophthalmol. Vis. Sci. 52, 9445–9451. https://doi.org/10.1167/iovs.11-7874.